
On Feature Diversity in Energy-based Models

Firas Laakom

Tampere University, Finland
firas.laakom@tuni.fi

Jenni Raitoharju

University of Jyväskylä, Finland
jenni.k.raitoharju@jyu.fi

Alexandros Iosifidis

Aarhus University, Denmark
ai@ece.au.dk

Moncef Gabbouj

Tampere University, Finland
moncef.gabbouj@tuni.fi

Abstract

Energy-based learning is a powerful learning paradigm that encapsulates various discriminative and generative approaches. An energy-based model (EBM) is typically formed of inner-model(s) that learn a combination of the different features to generate an energy mapping for each input configuration. In this paper, we focus on the diversity of the produced feature set. We extend the probably approximately correct (PAC) theory of EBMs and analyze the effect of redundancy reduction on the performance of EBMs. We derive generalization bounds for various learning contexts, i.e., regression, classification, and implicit regression, with different energy functions and we show that indeed reducing redundancy of the feature set can consistently decrease the gap between the true and empirical expectation of the energy and boosts the performance of the model.

1 Introduction

The energy-based learning paradigm was first proposed [1, 2] as an alternative to probabilistic graphical models [3]. As their name suggests, energy-based models (EBMs) map each input ‘configuration’ to a single scalar, called the ‘energy’. In the learning phase, the parameters of the model are optimized by associating the desired configurations with small energy values and the undesired ones with higher energy values [4–6]. In the inference phase, given an incomplete input configuration, the energy surface is explored to find the remaining variables which yield the lowest energy. EBMs encapsulate solutions to several supervised approaches [2, 7–10] and unsupervised learning problems [11–14] and provide a common theoretical framework for many learning models, including traditional discriminative [15, 16] and generative [1, 17–20] approaches.

Formally, let us denote the energy function by $E(h, \mathbf{x}, \mathbf{y})$, where $h = G_{\mathbf{W}}(\mathbf{x})$ represents the model with parameters \mathbf{W} to be optimized during training and \mathbf{x}, \mathbf{y} are sets of variables. Figure 1 illustrates how classification, regression, and implicit regression can be expressed as EBMs. In Figure 1 (a), a regression scenario is presented. The input \mathbf{x} , e.g., an image, is transformed using an inner model $G_{\mathbf{W}}(\mathbf{x})$ and its distance, to the second input \mathbf{y} is computed yielding the energy function. A valid energy function in this case can be the L_1 or the L_2 distance. In the binary classification case (Figure 1 (b)), the energy can be defined as $E(h, \mathbf{x}, \mathbf{y}) = -yG_{\mathbf{W}}(\mathbf{x})$. In the implicit regression case (Figure 1 (c)), we have two inner models and the energy can be defined as the L_2 distance between their outputs $E(h, \mathbf{x}, \mathbf{y}) = \frac{1}{2} \|G_{\mathbf{W}}^{(1)}(\mathbf{x}) - G_{\mathbf{W}}^{(2)}(\mathbf{y})\|_2^2$. In the inference phase, given an input \mathbf{x} , the label \mathbf{y}^* can be obtained by solving the following optimization problem:

$$\mathbf{y}^* = \arg \min_{\mathbf{y}} E(h, \mathbf{x}, \mathbf{y}). \quad (1)$$

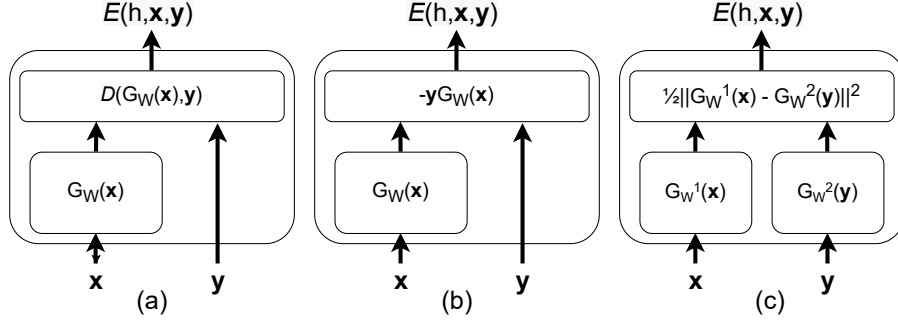


Figure 1: An illustration of energy-based models used to solve (a) a regression problem (b) a binary classification problem (c) an implicit regression problem.

An EBM typically relies on an inner model, i.e., $G_{\mathcal{W}}(\mathbf{x})$, to generate the desired energy landscape [2]. Depending on the problem at hand, this function can be constructed as a linear projection, a kernel method, or a neural network and its parameters are optimized in a data-driven manner in the training phase. Formally, $G_{\mathcal{W}}(\mathbf{x})$ can be written as

$$G_{\mathcal{W}}(\mathbf{x}) = \sum_i^D w_i \phi_i(\mathbf{x}), \quad (2)$$

where $\{\phi_1(\cdot), \dots, \phi_D(\cdot)\}$ is the feature set, which can be hand-crafted, separately trained from unlabeled data [21], or modeled by a neural network and optimized in the training phase of the EBM model [22–24]. In the rest of the paper, we assume that the inner models $G_{\mathcal{W}}$ defined in the energy-based learning system (Figure 1) are obtained as a weighted sum of different features as expressed in equation 2.

In [25], it was shown that simply minimizing the empirical energy over the training data does not theoretically guarantee the minimization of the expected value of the true energy. Thus, developing and motivating novel regularization techniques is required [21]. We argue that the quality of the feature set $\{\phi_1(\cdot), \dots, \phi_D(\cdot)\}$ plays a critical role in the overall performance of the global model. In this work, we extend the theoretical analysis of [25] and focus on the ‘diversity’ of this set and its effect on the generalization ability of the EBM models. Intuitively, it is clear that a less correlated set of intermediate representations is richer and thus able to capture more complex patterns in the input. Thus, it is important to avoid redundant features for achieving a better performance. However, a theoretical analysis is missing. We start by quantifying the diversity of a set of feature functions. To this end, we introduce $\vartheta - \tau$ -diversity:

Definition 1 ($(\vartheta - \tau)$ -diversity). *A set of feature functions, $\{\phi_1(\cdot), \dots, \phi_D(\cdot)\}$ is called ϑ -diverse, if there exists a constant $\vartheta \in \mathbb{R}$, such that for every input \mathbf{x} we have*

$$\frac{1}{2} \sum_{i \neq j}^D (\phi_i(\mathbf{x}) - \phi_j(\mathbf{x}))^2 \geq \vartheta^2 \quad (3)$$

with a high probability τ .

Intuitively, if two feature maps $\phi_i(\cdot)$ and $\phi_j(\cdot)$ are non-redundant, they have different outputs for the same input with a high probability. However, if, for example, the features are extracted using a neural network with a ReLU activation function, there is a high probability that some of the features associated with the input will be zero. Thus, defining a lower bound for the pair-wise diversity directly is impractical. Therefore, we quantify diversity as the lower-bound over the sum of the pair-wise distances of the feature maps as expressed in equation 3 and ϑ measures the diversity of a set.

In machine learning context, diversity has been explored in ensemble learning [26–28], sampling [29, 30], ranking [31, 32], pruning [33, 34], and neural networks [35–38]. In [35, 39], it was shown theoretically and experimentally that avoiding redundancy over the weights of a neural network using the mutual angles as a diversity measure improves the generalization ability of the model. In this work, we explore a new line of research, where diversity is defined over the feature maps directly,

using the $(\vartheta - \tau)$ -diversity, in the context of energy-based learning. In [18], a similar idea was empirically explored. A “repelling regularizer” was proposed to force non-redundant or orthogonal feature representations. Moreover, the idea of learning while avoiding redundancy has been used recently in the context of semi-supervised learning [40, 41]. Reducing redundancy by minimizing the cross-correlation of features learned using a Siamese network [40] was empirically shown to improve the generalization ability, yet a theoretical analysis to prove this has so far been lacking.

In this paper, we close the gap between empirical experience and theory. We theoretically study the generalization ability of EBMs in different learning contexts, i.e., regression, classification, implicit regression, and we derive new generalization bounds using the $(\vartheta - \tau)$ -diversity. In particular, we show that the generalization bound scales as $\mathcal{O}(\sqrt{DA^2 - \vartheta^2})$, where A is the maximum L_2 norm of the feature vector and ϑ is the features’ diversity. As the bound is inversely proportional ϑ , This shows that avoiding redundancy indeed improves the generalization ability of the model. The contributions of this paper can be summarized as follows:

- We explore a new line of research, where diversity is defined over the features representing the input data and not over the model’s parameters. To this end, we introduce $(\vartheta - \tau)$ -diversity as a quantification of the diversity of a given feature set.
- We extend the theoretical analysis [25] and study the effect of avoiding redundancy of a feature set on the generalization of EBMs.
- We derive bounds for the expectation of the true energy in different learning contexts, i.e., regression, classification, and implicit regression, using different energy functions. Our analysis consistently shows that avoiding redundancy by increasing the diversity of the feature set can boost the performance of an EBM.

2 PAC-learning of EBMs With $(\vartheta - \tau)$ -diversity

In this section, we derive a qualitative justification for $(\vartheta - \tau)$ -diversity using probably approximately correct (PAC) learning [42–44]. The PAC-based theory for standard EBMs has been established in [25]. First, we start by defining Rademacher complexity:

Definition 2. [43, 45] For a given dataset with m samples $\mathcal{S} = \{\mathbf{x}_i, y_i\}_{i=1}^m$ from a distribution \mathcal{D} and for a model space $\mathcal{F} : \mathcal{X} \rightarrow \mathbb{R}$ with a single dimensional output, the Empirical Rademacher complexity $\hat{\mathcal{R}}_m(\mathcal{F})$ of the set \mathcal{F} is defined as follows:

$$\hat{\mathcal{R}}_m(\mathcal{F}) = \mathbb{E}_\sigma \left[\sup_{f \in \mathcal{F}} \frac{1}{m} \sum_{i=1}^m \sigma_i f(\mathbf{x}_i) \right], \quad (4)$$

where the Rademacher variables $\sigma = \{\sigma_1, \dots, \sigma_m\}$ are independent uniform random variables in $\{-1, 1\}$.

The Rademacher complexity $\mathcal{R}_m(\mathcal{F})$ is defined as the expectation of the Empirical Rademacher complexity over training set, i.e., $\mathcal{R}_m(\mathcal{F}) = \mathbb{E}_{\mathcal{S} \sim \mathcal{D}^m} [\hat{\mathcal{R}}_m(\mathcal{F})]$. Based on this quantity, [45], several learning guarantees for EBMs have been shown [25]. We recall the following two lemmas related to the estimation error and the Rademacher complexity. In Lemma 1, we review the main PAC-learning bound for EBMs with finite outputs.

Lemma 1. [25] For a well-defined energy function $E(h, \mathbf{x}, \mathbf{y})$ over hypothesis class \mathcal{H} , input set \mathcal{X} and output set \mathcal{Y} , the following holds for all h in \mathcal{H} with a probability of at least $1 - \delta$

$$\mathbb{E}_{(\mathbf{x}, \mathbf{y}) \sim \mathcal{D}} [E(h, \mathbf{x}, \mathbf{y})] \leq \frac{1}{m} \sum_{(\mathbf{x}, \mathbf{y}) \in \mathcal{S}} E(h, \mathbf{x}, \mathbf{y}) + 2\mathcal{R}_m(\mathcal{E}) + M \sqrt{\frac{\log(2/\delta)}{2m}}, \quad (5)$$

where \mathcal{E} is the energy function class defined as $\mathcal{E} = \{E(h, \mathbf{x}, \mathbf{y}) | h \in \mathcal{H}\}$, $\mathcal{R}_m(\mathcal{E})$ is its Rademacher complexity, and M is the upper bound of \mathcal{E} .

Lemma 1 provides a generalization bound for EBMs with well-defined (non-negative) and bounded energy. The expected energy is bounded using the sum of three terms: The first term is the empirical expectation of energy over the training data, the second term depends on the Rademacher complexity of the energy class, and the third term involves the number of the training data m and the upper-bound

of the energy function M . This shows that merely minimizing the empirical expectation of energy, i.e., the first term, may not yield a good approximation of the true expectation. In [21], it has been shown that regularization using unlabeled data reduces the second and third terms leading to better generalization.

In this work, we express these two terms using the $(\vartheta - \tau)$ -diversity and show that employing a diversity strategy may also decrease the gap between the true and empirical expectation of the energy. In Section 2.1, we consider the special case of regression and derive two bounds for two energy functions based on L_1 and L_2 distances. In Section 2.2, we derive a bound for the binary classification task using as energy function $E(h, \mathbf{x}, \mathbf{y}) = -yG_{\mathbf{W}}(\mathbf{x})$ [2]. In Section 2.3, we consider the case of implicit regression, which encapsulates different learning problems such as metric learning, generative models, and denoising [2]. For this case, we use the L_2 distance between the inner models as the energy function. In the rest of the paper, we denote the generalization gap, $\mathbb{E}_{(\mathbf{x}, \mathbf{y}) \sim D}[E(h, \mathbf{x}, \mathbf{y})] - \frac{1}{m} \sum_{(\mathbf{x}, \mathbf{y}) \in S} E(h, \mathbf{x}, \mathbf{y})$ by $\Delta_{D, S} E$. All the proofs are presented in the supplementary material.

2.1 Regression Task

Regression can be formulated as an energy-based learning problem [8–10] (Figure 1 (a)) using the inner model $h(\mathbf{x}) = G_{\mathbf{W}}(\mathbf{x}) = \sum_{i=1}^D w_i \phi_i(\mathbf{x}) = \mathbf{w}^T \Phi(\mathbf{x})$. We assume that the feature set is positive and well-defined over the input domain \mathcal{X} , i.e., $\forall \mathbf{x} \in \mathcal{X} : \|\Phi(\mathbf{x})\|_2 \leq A$, the hypothesis class can be defined as follows: $\mathcal{H} = \{h(\mathbf{x}) = G_{\mathbf{W}}(\mathbf{x}) = \sum_{i=1}^D w_i \phi_i(\mathbf{x}) = \mathbf{w}^T \Phi(\mathbf{x}) \mid \Phi \in \mathcal{F}, \forall \mathbf{x} : \|\Phi(\mathbf{x})\|_2 \leq A\}$, the output set $\mathcal{Y} \subset \mathbb{R}$ is bounded, i.e., $y < B$, and the feature set $\{\phi_1(\cdot), \dots, \phi_D(\cdot)\}$ is ϑ -diverse with a probability τ . The two valid energy functions which can be used for regression are $E_2(h, \mathbf{x}, \mathbf{y}) = \frac{1}{2} \|G_{\mathbf{W}}(\mathbf{x}) - y\|_2^2$ and $E_1(h, \mathbf{x}, \mathbf{y}) = \|G_{\mathbf{W}}(\mathbf{x}) - y\|_1$ [2]. We study these two cases separately and we show theoretically that for both energy functions avoiding redundancy improves generalization of the EBM model.

Energy Function: E_2

In this subsection, we present our theoretical analysis on the effect of diversity on the generalization ability of an EBM defined with the energy function $E_2(h, \mathbf{x}, \mathbf{y}) = \frac{1}{2} \|G_{\mathbf{W}}(\mathbf{x}) - y\|_2^2$. We start by the following two Lemmas 2 and 3.

Lemma 2. *With a probability of at least τ , we have*

$$\sup_{\mathbf{x}, \mathbf{W}} |h(\mathbf{x})| \leq \|\mathbf{w}\|_{\infty} \sqrt{(DA^2 - \vartheta^2)}. \quad (6)$$

Lemma 3. *With a probability of at least τ , we have*

$$\sup_{\mathbf{x}, \mathbf{y}, h} |E(h, \mathbf{x}, \mathbf{y})| \leq \frac{1}{2} (\|\mathbf{w}\|_{\infty} \sqrt{(DA^2 - \vartheta^2)} + B)^2. \quad (7)$$

Lemmas 2 and 3 bound the supremum of the output of the inner model and the energy function as a function of ϑ , respectively. As it can be seen, both terms are decreasing with respect to diversity. Next, we bound the Rademacher complexity of the energy class, i.e., $\mathcal{R}_m(\mathcal{E})$.

Lemma 4. *With a probability of at least τ , we have*

$$\mathcal{R}_m(\mathcal{E}) \leq 2D \|\mathbf{w}\|_{\infty} (\|\mathbf{w}\|_{\infty} \sqrt{(DA^2 - \vartheta^2)} + B) \mathcal{R}_m(\mathcal{F}). \quad (8)$$

Lemma 4 expresses the bound of the Rademacher complexity of the energy class using the diversity constant and the Rademacher complexity of the features. Having expressed the different terms of Lemma 1 using diversity, we now present our main result for an energy-based model trained defined using E_2 . The main result is presented in Theorem 1.

Theorem 1. *For the energy function $E(h, \mathbf{x}, \mathbf{y}) = \frac{1}{2} \|G_{\mathbf{W}}(\mathbf{x}) - y\|_2^2$, over the input set $\mathcal{X} \in \mathbb{R}^N$, hypothesis class $\mathcal{H} = \{h(\mathbf{x}) = G_{\mathbf{W}}(\mathbf{x}) = \sum_{i=1}^D w_i \phi_i(\mathbf{x}) = \mathbf{w}^T \Phi(\mathbf{x}) \mid \Phi \in \mathcal{F}, \forall \mathbf{x} : \|\Phi(\mathbf{x})\|_2 \leq A\}$, and output set $\mathcal{Y} \subset \mathbb{R}$, if the feature set $\{\phi_1(\cdot), \dots, \phi_D(\cdot)\}$ is ϑ -diverse with a probability τ , with a probability of at least $(1 - \delta)\tau$, the following holds for all h in \mathcal{H} :*

$$\Delta_{D, S} E \leq 4D \|\mathbf{w}\|_{\infty} (\|\mathbf{w}\|_{\infty} \sqrt{DA^2 - \vartheta^2} + B) \mathcal{R}_m(\mathcal{F}) + \frac{1}{2} (\|\mathbf{w}\|_{\infty} \sqrt{DA^2 - \vartheta^2} + B)^2 \sqrt{\frac{\log(2/\delta)}{2m}}, \quad (9)$$

where B is the upper-bound of \mathcal{Y} , i.e., $y \leq B, \forall y \in \mathcal{Y}$.

Theorem 1 express the special case of Lemma 1 using the $(\vartheta - \tau)$ -diversity of the feature set $\{\phi_1(\cdot), \dots, \phi_D(\cdot)\}$. As it can be seen, the bound of the generalization error is inversely proportional to ϑ^2 . This theoretically shows that reducing redundancy, i.e., increasing ϑ , reduces the gap between the true and the empirical energies and improves the generalization performance of the EBMs.

Energy Function: E_1

In this subsection, we consider the second case of regression using the energy function $E_1(h, \mathbf{x}, \mathbf{y}) = \|G_{\mathbf{W}}(\mathbf{x}) - y\|_1$. Similar to the previous case, we start by deriving bounds for the energy function and the Rademacher complexity of the class using diversity in Lemmas 5 and 6.

Lemma 5. *With a probability of at least τ , we have*

$$\sup_{\mathbf{x}, y, h} |E(h, \mathbf{x}, \mathbf{y})| \leq (\|\mathbf{w}\|_{\infty} \sqrt{DA^2 - \vartheta^2} + B). \quad (10)$$

Lemma 6. *With a probability of at least τ , we have*

$$\mathcal{R}_m(\mathcal{E}) \leq 2D\|\mathbf{w}\|_{\infty} \mathcal{R}_m(\mathcal{F}). \quad (11)$$

Next, we derive the main result of the generalization of the EBMs defined using the energy function E_1 . The main finding is presented in Theorem 2.

Theorem 2. *For the energy function $E(h, \mathbf{x}, \mathbf{y}) = \|G_{\mathbf{W}}(\mathbf{x}) - y\|_1$, over the input set $\mathcal{X} \in \mathbb{R}^N$, hypothesis class $\mathcal{H} = \{h(\mathbf{x}) = G_{\mathbf{W}}(\mathbf{x}) = \sum_{i=1}^D w_i \phi_i(\mathbf{x}) = \mathbf{w}^T \Phi(\mathbf{x}) \mid \Phi \in \mathcal{F}, \forall \mathbf{x} \|\Phi(\mathbf{x})\|_2 \leq A\}$, and output set $\mathcal{Y} \subset \mathbb{R}$, if the feature set $\{\phi_1(\cdot), \dots, \phi_D(\cdot)\}$ is ϑ -diverse with a probability τ , then with a probability of at least $(1 - \delta)\tau$, the following holds for all h in \mathcal{H} :*

$$\Delta_{D,S} E \leq 4D\|\mathbf{w}\|_{\infty} \mathcal{R}_m(\mathcal{F}) + (\|\mathbf{w}\|_{\infty} \sqrt{DA^2 - \vartheta^2} + B) \sqrt{\frac{\log(2/\delta)}{2m}}, \quad (12)$$

where B is the upper-bound of \mathcal{Y} , i.e., $y \leq B, \forall y \in \mathcal{Y}$.

Similar to Theorem 1, in Theorem 2, we consistently find that the bound of the true expectation of the energy is a decreasing function with respect to ϑ . This proves that for the regression task reducing redundancy can improve the generalization performance of the energy-based model.

2.2 Binary Classifier

Here, we consider the problem of binary classification, as illustrated in Figure 1 (b). Using the same assumption as in regression for the inner model, i.e., $h(\mathbf{x}) = G_{\mathbf{W}}(\mathbf{x}) = \sum_{i=1}^D w_i \phi_i(\mathbf{x}) = \mathbf{w}^T \Phi(\mathbf{x})$, energy function of $E(h, \mathbf{x}, \mathbf{y}) = -yG_{\mathbf{W}}(\mathbf{x})$ [2], and the $(\vartheta - \tau)$ -diversity of the feature set, we express Lemma 1 for this specific configuration in Theorem 3.

Theorem 3. *For the energy function $E(h, \mathbf{x}, \mathbf{y}) = -yG_{\mathbf{W}}(\mathbf{x})$, over the input set $\mathcal{X} \in \mathbb{R}^N$, hypothesis class $\mathcal{H} = \{h(\mathbf{x}) = G_{\mathbf{W}}(\mathbf{x}) = \sum_{i=1}^D w_i \phi_i(\mathbf{x}) = \mathbf{w}^T \Phi(\mathbf{x}) \mid \Phi \in \mathcal{F}, \forall \mathbf{x} : \|\Phi(\mathbf{x})\|_2 \leq A\}$, and output set $\mathcal{Y} \subset \mathbb{R}$, if the feature set $\{\phi_1(\cdot), \dots, \phi_D(\cdot)\}$ is ϑ -diverse with a probability τ , then with a probability of at least $(1 - \delta)\tau$, the following holds for all h in \mathcal{H} :*

$$\Delta_{D,S} E \leq 4D\|\mathbf{w}\|_{\infty} \mathcal{R}_m(\mathcal{F}) + \|\mathbf{w}\|_{\infty} \sqrt{DA^2 - \vartheta^2} \sqrt{\frac{\log(2/\delta)}{2m}}. \quad (13)$$

Similar to the regression task, we note that the upper-bound of the true expectation is a decreasing function with respect to the diversity term. Thus, a less redundant feature set, i.e., higher ϑ , has a lower upper-bound for the true energy.

2.3 Implicit Regression

In this section, we consider the problem of implicit regression. This is a general formulation of a different set of problems such as metric learning, where the goal is to learn a distance function between

two domains, image denoising, object detection as illustrated in [2], or semi-supervised learning [40]. This form of EBM (Figure 1 (c)) has two inner models, $G_{\mathbf{W}}^1(\cdot)$ and $G_{\mathbf{W}}^2(\cdot)$, which can be equal or different according to the problem at hand. Here, we consider the general case, where the two models correspond to two different combinations of different features, i.e., $G_{\mathbf{W}}^1(\mathbf{x}) = \sum_{i=1}^{D^{(1)}} w_i^{(1)} \phi_i^{(1)}(\mathbf{x})$ and $G_{\mathbf{W}}^2(\mathbf{y}) = \sum_{i=1}^{D^{(2)}} w_i^{(2)} \phi_i^{(2)}(\mathbf{y})$. Thus, we have a different $(\vartheta - \tau)$ -diversity term for each set. The final result is presented in Theorem 4.

Theorem 4. *For the energy function $E(h, \mathbf{x}, \mathbf{y}) = \frac{1}{2} \|G_{\mathbf{W}}^1(\mathbf{x}) - G_{\mathbf{W}}^2(\mathbf{y})\|_2^2$, over the input set $\mathcal{X} \in \mathbb{R}^N$, hypothesis class $\mathcal{H} = \{h^{(1)}(\mathbf{x}) = G_{\mathbf{W}}^1(\mathbf{x}) = \sum_{i=1}^{D^{(1)}} w_i^{(1)} \phi_i^{(1)}(\mathbf{x}) = \mathbf{w}^{(1)T} \Phi^{(1)}(\mathbf{x}), h^{(2)}(\mathbf{x}) = G_{\mathbf{W}}^2(\mathbf{y}) = \sum_{i=1}^{D^{(2)}} w_i^{(2)} \phi_i^{(2)}(\mathbf{y}) = \mathbf{w}^{(2)T} \Phi^{(2)}(\mathbf{y}) \mid \Phi^{(1)} \in \mathcal{F}_1, \Phi^{(2)} \in \mathcal{F}_2, \forall \mathbf{x} : \|\Phi^{(1)}(\mathbf{x})\|_2 \leq A^{(1)}, \forall \mathbf{y} : \|\Phi^{(2)}(\mathbf{y})\|_2 \leq A^{(2)}\}$, and output set $\mathcal{Y} \subset \mathbb{R}^N$, if the feature set $\{\phi_1^{(1)}(\cdot), \dots, \phi_{D^{(1)}}^{(1)}(\cdot)\}$ is $\vartheta^{(1)}$ -diverse with a probability τ_1 and the feature set $\{\phi_1^{(2)}(\cdot), \dots, \phi_{D^{(2)}}^{(2)}(\cdot)\}$ is $\vartheta^{(2)}$ -diverse with a probability τ_2 , then with a probability of at least $(1 - \delta)\tau_1\tau_2$, the following holds for all h in \mathcal{H} :*

$$\Delta_{D,SE} \leq 8(\sqrt{\mathcal{J}_1} + \sqrt{\mathcal{J}_2}) \left(D^{(1)} \|\mathbf{w}^{(1)}\|_{\infty} \mathcal{R}_m(\mathcal{F}_1) + D^{(2)} \|\mathbf{w}^{(2)}\|_{\infty} \mathcal{R}_m(\mathcal{F}_2) \right) + (\mathcal{J}_1 + \mathcal{J}_2) \sqrt{\frac{\log(2/\delta)}{2m}}, \quad (14)$$

where $\mathcal{J}_1 = \|\mathbf{w}^{(1)}\|_{\infty}^2 (D^{(1)} A^{(1)2} - \vartheta^{(1)2})$ and $\mathcal{J}_2 = \|\mathbf{w}^{(2)}\|_{\infty}^2 (D^{(2)} A^{(2)2} - \vartheta^{(2)2})$.

The upper-bound of the energy model depends on the diversity variable of both feature sets. Moreover, we note that the bound for the implicit regression decreases proportionally to ϑ^2 , as opposed to the classification case for example, where the bound is proportional to ϑ . Thus, we can conclude that reducing redundancy improves the generalization of EBM in the implicit regression context.

2.4 General Discussion

We note that the theory developed in our paper (Theorems 1 to 4) is agnostic to the loss function [2] or the optimization strategy used [4, 5, 14, 23]. We show that reducing the redundancy of the features consistently decreases the upper-bound of the true expectation of the energy and, thus, can boost the generalization performance of the energy-based model. We also note that our analysis is independent of how the features are obtained, e.g., handcrafted or optimized. In fact, in the recent state-of-the-art EBMs [12, 20, 23], the features are typically parameterized using a deep learning model and optimized during training.

We note that our $(\vartheta - \tau)$ -diversity is not scale invariant, i.e., it is sensitive to the L_2 -norm of the feature vector A . This suggests that one might reduce $(\vartheta - \tau)$ -diversity by controlling the feature norm without affecting the true redundancy of the features. However, our bound can be interpreted as follows: 'Given two models with the same value of A (maximum L_2 -norm of the features), the model with higher diversity ϑ has a lower generalization bound and is likely to generalize better'. From this perspective, our findings remain valid showing that reducing redundancy, i.e., increasing ϑ , reduces the gap between the true and the empirical energies and improves the generalization performance of the EBMs.

Our contribution is twofold. First, we provide theoretical guarantees that reducing redundancy in the feature space can indeed improve the generalization of the EBM. This can pave the way toward providing theoretical guarantees for works on self-supervised learning using redundancy reduction [40, 41, 18]. Second, our theory can be used to motivate novel redundancy reduction strategies, for example, in the form of regularization [38], to avoid learning redundant features. Such strategies can improve the performance of the model and improve generalization.

3 Simple Regularization Algorithm

In general, theoretical generalization bounds can be too loose to be direct practical implications [46, 47]. However, they typically suggest a regularizer to promote some desired aspects of the hypothesis class [35, 44, 48]. Accordingly, inspired by the theoretical analysis in Section 2, we propose a straightforward strategy to avoid learning redundant features by regularizing the model

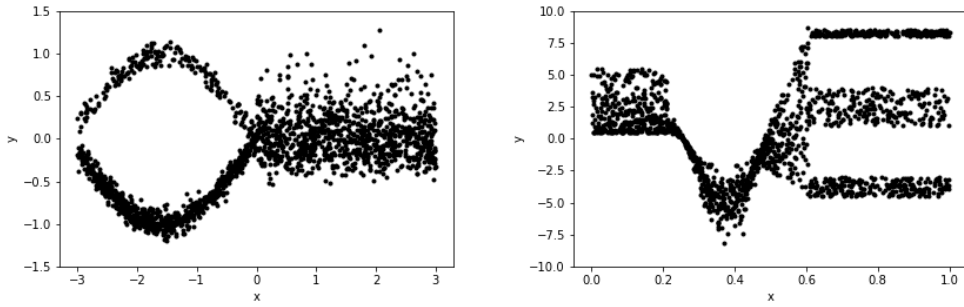


Figure 2: Visualization of the training data for the 1-D regression tasks: The dataset [9] on the left and the dataset [49] on the right.

during the training using a term inversely proportional to $\vartheta - \tau$ -diversity of the features. Given an EBM model with a learnable feature set $\{\phi_1(\cdot), \dots, \phi_D(\cdot)\}$ and a training set S , we propose to augment the original training loss L as follows:

$$L_{aug} = L - \beta \sum_{\mathbf{x} \in S} \sum_{i \neq j}^D (\phi_i(\mathbf{x}) - \phi_j(\mathbf{x}))^2, \quad (15)$$

where β is a hyper-parameter controlling the contribution of the second term in the total loss. The additional term penalizes the similarities between the distinct features ensuring learning a diverse and non-redundant mapping of the data. As a result, this can improve the general performance of our model.

3.1 Regression Task

Recently, there has been a high interest in using EBMs to solve regression tasks [8–10]. As shown in Section 2.1, learning diverse features yields better generalization. In this subsection, we validate the proposed regularizer equation 15 on two 1-D regression tasks. For the first task, we use the dataset proposed in [9], which has 2 000 training examples. The training data of this dataset is visualized in Figure 2 (left). For the second task, similar to [8], we use the regression dataset proposed in [49], containing 1900 test examples and 1700 examples for training. The training data of this dataset is visualized in Figure 2 (right).

To train EBMs for regression tasks, several losses has been proposed [10, 50, 51]. In this work, similar to [9], we use the noise contrastive estimation (NCE) loss [51] with the noise distribution

$$q(y) = \frac{1}{2} \sum_{j=1}^2 \mathcal{N}(y; y_j, \sigma_j^2 \mathbf{I}), \quad (16)$$

where σ_1 and σ_2 are two hyperparameters. As suggested in [8, 9], we set $\sigma_2 = 8\sigma_1$ in all experiments. We evaluate the performance of our approach by augmenting the NCE loss using equation 15 to penalize the feature redundancy.

We follow the same experimental setup used in [8, 9]. The inner model (Figure 1) of X is formed by a fully-connected network with 2 hidden layers followed by Relu activations. We consider as 'features' for computing our regularizer, the output of this inner model. The input y is also processed with one fully-connected layer with 10 units followed by Relu. Additionally, the concatenated outputs of both models is passed through a network composed of four hidden layers. All hidden layers are formed of 10 units except the final output, which has one hidden units corresponding to the predicted energy. The model is trained in an end-to-end manner for 75 epochs with Adam optimizer [52] with a learning rate of 0.001. Similar to [8, 9], the batch size is selected to be 32 and the number of samples M is always set to $M = 1024$.

For the evaluation, we follow the standard protocol of these two datasets: For the first one, we evaluate the approaches using KL divergence [8, 9]. For the second dataset, we report the NLL

results as proposed in [8, 49]. Moreover, we report the results for several noise distributions of NCE: $\sigma_1 \in \{0.05, 0.1, 0.2\}$. The average experimental results over 20 random seeds for different values of β are reported in Table 1. As it can be seen, avoiding feature redundancy consistently boosts the performance of the EBM model for both datasets and all different values of σ_1 .

Approach	Dataset [9]			Dataset [49]		
	$\sigma_1 = 0.05$	$\sigma_1 = 0.1$	$\sigma_1 = 0.2$	$\sigma_1 = 0.05$	$\sigma_1 = 0.1$	$\sigma_1 = 0.2$
EBM	0.0445	0.0420	0.0374	2.7776	2.5650	1.9876
ours ($\beta = 1e^{-11}$)	0.0398	0.3450	0.0357	2.6187	2.4414	1.8072
ours ($\beta = 1e^{-12}$)	0.0409	0.0380	0.0343	2.5846	2.36853	1.8880
ours ($\beta = 1e^{-13}$)	0.0410	0.0332	0.0377	2.7483	2.5420	1.9303

Table 1: Results of the EBM trained with NCE (EBM) and the EBM trained with NCE augmented with our regularizer (ours) for the 1-D regression tasks. Results are in terms of approximate KL divergence for the first dataset [9], and in terms of approximate NLL for the second dataset [49]. For each dataset, we report the results for three different values of σ_1 , the hyperparameter of NCE.

3.2 Continual Learning

In this subsection, we validate the proposed regularizer on a more challenging task, namely the Continual Learning (CL) problem. CL tackles the problem of catastrophic forgetting in deep learning models [53–55]. Its main goal is to solve several tasks sequentially without forgetting knowledge learned from the past. So, a continual learner is expected to learn a new task, crucially, without forgetting previous tasks. Recently, an EBM-based CL approach was proposed in [16] and led to superior results compared to standard approaches.

For this experiment, we use the same models and the same experimental protocol used in [16]. However, here we focus only on the class-incremental learning task using CIFAR10 and CIFAR100. We evaluate the performance of our proposed regularizer using both the boundary-aware and boundary-agnostic settings. As defined in [16], the boundary-aware refers to the situation where the sequence of the tasks has explicit separation between them which is known to the model. The boundary agnostic case refers to the situation where the data distributions gradually changes without a notion of task boundaries.

We consider as ‘features’ the representation obtained by the last intermediate layer. The proposed regularizer is applied on top of this representation. In Table 2, we report the performance of the EBM trained using the original loss and using the loss augmented with our additional term for different values of β . As shown in Table 2, penalizing feature similarity and promoting the diversity of the feature set boosts the performance of the EBM model and consistently leads to a superior accuracy for both datasets. In Figure 3, we display the accumulated classification accuracy, averaged over tasks, on the test set. Along the five tasks, our approach maintains higher classification accuracy than the standard EBM for both the boundary-aware and boundary-agnostic settings.

It should be noted here that the regularizer is just an example showing how our theory can be used in practice. Thus, when we defined the regularizer, we tried to stay as close as possible to the $(\vartheta - \tau)$ -diversity definition (Definition 1). We used directly the definition of diversity as a regularizer

Method	Boundary-aware		Boundary-agnostic	
	CIFAR10	CIFAR100	CIFAR10	CIFAR100
EBM	39.15 \pm 0.86	29.02 \pm 0.24	48.40 \pm 0.80	34.78 \pm 0.26
ours ($\beta = 1e^{-11}$)	39.61 \pm 0.81	29.15 \pm 0.27	49.63 \pm 0.90	34.86 \pm 0.30
ours ($\beta = 1e^{-12}$)	40.64 \pm 0.79	29.38 \pm 0.21	50.25 \pm 0.63	35.20 \pm 0.23
ours ($\beta = 1e^{-13}$)	40.15 \pm 0.87	29.28 \pm 0.28	50.20 \pm 0.94	35.03 \pm 0.21

Table 2: Evaluation of class-incremental learning on both the boundary-aware and boundary-agnostic setting on CIFAR10 and CIFAR100 datasets. Each experiment was performed ten times with different random seeds, the results are reported as the mean/SEM over these runs.

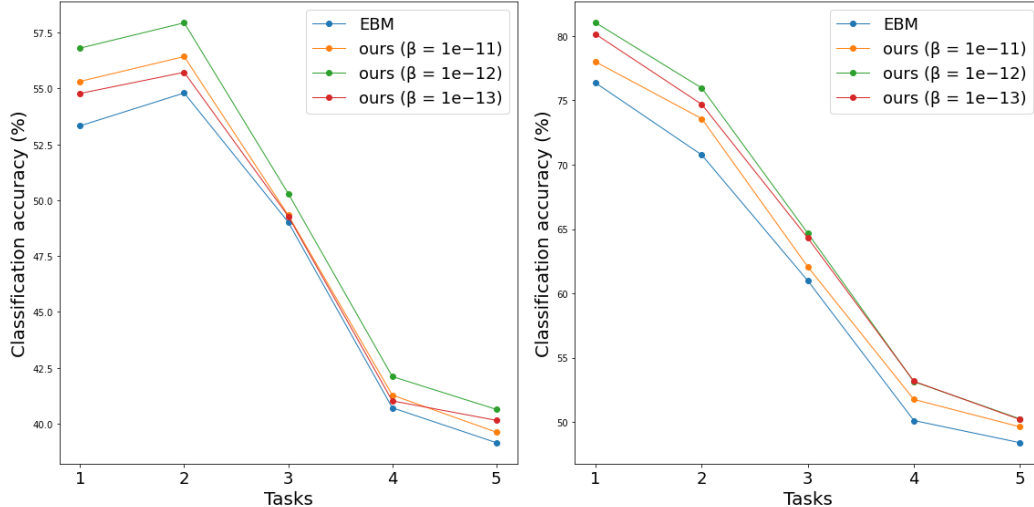


Figure 3: Average test classification accuracy vs number of observed tasks on CIFAR10 using the boundary-aware (left) and boundary-agnostic (right) setting. The results are averaged over ten random seeds.

(equation 15). It contains two sums: the first sum is over the whole batch and the second sum is over all pairs of units within the layers. This yields a total of ND^2 terms, where N is the batch size and D is the number of units within the layer. This results in empirically large values of the second term ($\sim 10^9$). Thus, β needs to be small so the loss is not dominated by the second term. Empirically, we found that $[10^{-11}, 10^{-13}]$ corresponds to a stable range.

4 Conclusion

Energy-based learning is a powerful learning paradigm that encapsulates various discriminative and generative systems. An EBM is typically formed of one (or many) inner models which learn a combination of different features to generate an energy mapping for each input configuration. In this paper, we introduced a feature diversity concept, i.e., $(\vartheta - \tau)$ -diversity, and we used it to extend the PAC theory of EBMs. We derived different generalization bounds for various learning contexts, i.e., regression, classification, and implicit regression, with different energy functions. We consistently found that reducing the redundancy of the feature set can improve the generalization error of energy-based approaches. We also note that our theory is independent of the loss function or the training strategy used to optimize the parameters of the EBM. This provides theoretical guarantees on learning via feature redundancy reduction. Our preliminary experimental results confirm that this is indeed a promising research direction and can motivate the development of novel approaches to promote the diversity of the feature set. Future directions include more extensive experimental evaluation of different feature redundancy reduction approaches.

Acknowledgments and Disclosure of Funding

This work was supported by NSF-Business Finland Center for Visual and Decision Informatics (CVDI) project AMALIA.

References

- [1] Song Chun Zhu and David Mumford. Grade: Gibbs reaction and diffusion equations. In *Sixth International Conference on Computer Vision (IEEE Cat. No. 98CH36271)*, pages 847–854. IEEE, 1998.
- [2] Yann LeCun, Sumit Chopra, Raia Hadsell, M Ranzato, and F Huang. A tutorial on energy-based learning. *Predicting structured data*, 1, 2006.

- [3] Daphne Koller and Nir Friedman. *Probabilistic graphical models: principles and techniques*. MIT press, 2009.
- [4] Rithesh Kumar, Sherjil Ozair, Anirudh Goyal, Aaron Courville, and Yoshua Bengio. Maximum entropy generators for energy-based models. *arXiv preprint arXiv:1901.08508*, 2019.
- [5] Yang Song and Stefano Ermon. Generative modeling by estimating gradients of the data distribution. In *Neurips*, 2019.
- [6] Xu Yang, Xin Geng, and Deyu Zhou. Sparsity conditional energy label distribution learning for age estimation. In *IJCAI*, 2016.
- [7] Yi Fang and Mengwen Liu. A unified energy-based framework for learning to rank. In *ACM International Conference on the Theory of Information Retrieval*, 2016.
- [8] Fredrik K Gustafsson, Martin Danelljan, and Thomas B Schön. Learning proposals for practical energy-based regression. In *Proceedings of the International Conference on Artificial Intelligence and Statistics (AISTATS)*, 2022.
- [9] Fredrik K Gustafsson, Martin Danelljan, Radu Timofte, and Thomas B Schön. How to train your energy-based model for regression. In *Proceedings of the British Machine Vision Conference (BMVC)*, 2020.
- [10] Fredrik K Gustafsson, Martin Danelljan, Goutam Bhat, and Thomas B Schön. Energy-based models for deep probabilistic regression. In *Proceedings of the European Conference on Computer Vision (ECCV)*, 2020.
- [11] Yuntian Deng, Anton Bakhtin, Myle Ott, Arthur Szlam, and Marc’Aurelio Ranzato. Residual energy-based models for text generation. *arXiv preprint arXiv:2004.11714*, 2020.
- [12] Anton Bakhtin, Yuntian Deng, Sam Gross, Myle Ott, Marc’Aurelio Ranzato, and Arthur Szlam. Residual energy-based models for text. *JMLR*, 2021.
- [13] Yang Zhao, Jianwen Xie, and Ping Li. Learning energy-based generative models via coarse-to-fine expanding and sampling. In *International Conference on Learning Representations*, 2020.
- [14] Yifei Xu, Jianwen Xie, Tianyang Zhao, Chris Baker, Yibiao Zhao, and Ying Nian Wu. Energy-based continuous inverse optimal control. *IEEE Transactions on Neural Networks and Learning Systems*, 2022.
- [15] Shuangfei Zhai, Yu Cheng, Weining Lu, and Zhongfei Zhang. Deep structured energy based models for anomaly detection. In *ICML*. PMLR, 2016.
- [16] Shuang Li, Yilun Du, Gido M van de Ven, Antonio Torralba, and Igor Mordatch. Energy-based models for continual learning. *arXiv preprint arXiv:2011.12216*, 2020.
- [17] Jianwen Xie, Song-Chun Zhu, and Ying Nian Wu. Synthesizing dynamic patterns by spatial-temporal generative convnet. In *Proceedings of the IEEE conference on computer vision and pattern recognition*, pages 7093–7101, 2017.
- [18] Junbo Zhao, Michael Mathieu, and Yann LeCun. Energy-based generative adversarial network. *ICLR*, 2017.
- [19] Tong Che, Ruixiang Zhang, Jascha Sohl-Dickstein, Hugo Larochelle, Liam Paull, Yuan Cao, and Yoshua Bengio. Your gan is secretly an energy-based model and you should use discriminator driven latent sampling. *arXiv preprint arXiv:2003.06060*, 2020.
- [20] Muhammad Khalifa, Hady Elsahar, and Marc Dymetman. A distributional approach to controlled text generation. *ICLR*, 2021.
- [21] Xiang Zhang and Yann LeCun. Universum prescription: Regularization using unlabeled data. In *AAAI*, 2017.

- [22] Jianwen Xie, Yang Lu, Song-Chun Zhu, and Yingnian Wu. A theory of generative convnet. In *International Conference on Machine Learning*, pages 2635–2644. PMLR, 2016.
- [23] Lantao Yu, Yang Song, Jiaming Song, and Stefano Ermon. Training deep energy-based models with f-divergence minimization. In *ICML*, 2020.
- [24] Jianwen Xie, Yifei Xu, Zilong Zheng, Song-Chun Zhu, and Ying Nian Wu. Generative pointnet: Deep energy-based learning on unordered point sets for 3d generation, reconstruction and classification. In *Proceedings of the IEEE/CVF Conference on Computer Vision and Pattern Recognition*, pages 14976–14985, 2021.
- [25] Xiang Zhang. *Pac-learning for energy-based models*. PhD thesis, Citeseer, 2013.
- [26] Nan Li, Yang Yu, and Zhi-Hua Zhou. Diversity regularized ensemble pruning. In *Joint European Conference on Machine Learning and Knowledge Discovery in Databases*, 2012.
- [27] Yang Yu, Yu-Feng Li, and Zhi-Hua Zhou. Diversity regularized machine. In *International Joint Conference on Artificial Intelligence*, 2011.
- [28] Jianxin Li, Haoyi Zhou, Pengtao Xie, and Yingchun Zhang. Improving the generalization performance of multi-class svm via angular regularization. In *IJCAI*, 2017.
- [29] Michal Dereziński, Daniele Calandriello, and Michal Valko. Exact sampling of determinantal point processes with sublinear time preprocessing. In *Advances in Neural Information Processing Systems*, 2019.
- [30] Erdem Bıyık, Kenneth Wang, Nima Anari, and Dorsa Sadigh. Batch active learning using determinantal point processes. *arXiv preprint arXiv:1906.07975*, 2019.
- [31] Qiong Wu, Yong Liu, Chunyan Miao, Binqiang Zhao, Yin Zhao, and Lu Guan. Pd-gan: Adversarial learning for personalized diversity-promoting recommendation. In *IJCAI*, 2019.
- [32] Lijing Qin and Xiaoyan Zhu. Promoting diversity in recommendation by entropy regularizer. In *IJCAI*, 2013.
- [33] Pravendra Singh, Vinay Kumar Verma, Piyush Rai, and Vinay Namboodiri. Leveraging filter correlations for deep model compression. In *The IEEE Winter Conference on Applications of Computer Vision*, 2020.
- [34] Seunghyun Lee, Byeongho Heo, Jung-Woo Ha, and Byung Cheol Song. Filter pruning and re-initialization via latent space clustering. *IEEE Access*, 8, 2020.
- [35] Pengtao Xie, Yuntian Deng, and Eric Xing. On the generalization error bounds of neural networks under diversity-inducing mutual angular regularization. *arXiv preprint arXiv:1511.07110*, 2015.
- [36] Dazhong Shen, Chuan Qin, Chao Wang, Hengshu Zhu, Enhong Chen, and Hui Xiong. Regularizing variational autoencoder with diversity and uncertainty awareness. In *IJCAI*, 2021.
- [37] Michael Cogswell, Faruk Ahmed, Ross B. Girshick, Larry Zitnick, and Dhruv Batra. Reducing overfitting in deep networks by decorrelating representations. In *International Conference on Learning Representations*, 2016.
- [38] Firas Laakom, Jenni Raitoharju, Alexandros Iosifidis, and Moncef Gabbouj. Wld-reg: A data-dependent within-layer diversity regularizer. In *AAAI*, 2023.
- [39] Bo Xie, Yingyu Liang, and Le Song. Diverse neural network learns true target functions. In *Artificial Intelligence and Statistics*, 2017.
- [40] Jure Zbontar, Li Jing, Ishan Misra, Yann LeCun, and Stéphane Deny. Barlow twins: Self-supervised learning via redundancy reduction. *ICML*, 2021.
- [41] Adrien Bardes, Jean Ponce, and Yann LeCun. Vicreg: Variance-invariance-covariance regularization for self-supervised learning. *arXiv preprint arXiv:2105.04906*, 2021.

- [42] Leslie G Valiant. A theory of the learnable. *Communications of the ACM*, 1984.
- [43] Mehryar Mohri, Afshin Rostamizadeh, and Ameet Talwalkar. *Foundations of machine learning*. MIT press, 2018.
- [44] Jian Li, Yong Liu, Rong Yin, and Weiping Wang. Multi-class learning using unlabeled samples: Theory and algorithm. In *IJCAI*, 2019.
- [45] Peter L Bartlett and Shahar Mendelson. Rademacher and gaussian complexities: Risk bounds and structural results. *JMLR*, 2002.
- [46] Chiyuan Zhang, Samy Bengio, Moritz Hardt, Benjamin Recht, and Oriol Vinyals. Understanding deep learning requires rethinking generalization. In *ICLR*, 2017.
- [47] Behnam Neyshabur, Srinadh Bhojanapalli, David McAllester, and Nathan Srebro. Exploring generalization in deep learning. *NIPS*, 2017.
- [48] Kenji Kawaguchi, Leslie Pack Kaelbling, and Yoshua Bengio. Generalization in deep learning. *arXiv preprint arXiv:1710.05468*, 2017.
- [49] Axel Brando, Jose A Rodriguez, Jordi Vitria, and Alberto Rubio Muñoz. Modelling heterogeneous distributions with an uncountable mixture of asymmetric laplacians. *Advances in neural information processing systems*, 32, 2019.
- [50] Aapo Hyvärinen and Peter Dayan. Estimation of non-normalized statistical models by score matching. *Journal of Machine Learning Research*, 6(4), 2005.
- [51] Michael Gutmann and Aapo Hyvärinen. Noise-contrastive estimation: A new estimation principle for unnormalized statistical models. In *Proceedings of the thirteenth international conference on artificial intelligence and statistics*, pages 297–304. JMLR Workshop and Conference Proceedings, 2010.
- [52] Ian Goodfellow, Yoshua Bengio, Aaron Courville, and Yoshua Bengio. *Deep learning*, volume 1. MIT Press, 2016.
- [53] German I. Parisi, Ronald Kemker, Jose L. Part, Christopher Kanan, and Stefan Wermter. Continual lifelong learning with neural networks: A review. *Neural Networks*, 2019.
- [54] Zhizhong Li and Derek Hoiem. Learning without forgetting. *IEEE TPAMI*, 2017.
- [55] Takashi Shibata, Go Irie, Daiki Ikami, and Yu Mitsuzumi. Learning with selective forgetting. In *IJCAI*, 2021.
- [56] Michael M Wolf. *Mathematical foundations of supervised learning*, 2018.
- [57] Yilun Du and Igor Mordatch. Implicit generation and modeling with energy based models. In *Advances in Neural Information Processing Systems*, 2019.
- [58] Yilun Du, Shuang Li, Joshua Tenenbaum, and Igor Mordatch. Improved contrastive divergence training of energy-based models. In *Proceedings of the 38th International Conference on Machine Learning*, 2021.
- [59] Deep energy-based generative models. https://uvadlc-notebooks.readthedocs.io/en/latest/tutorial_notebooks/tutorial8/Deep_Energy_Models.html. Accessed: 2022-05-01.
- [60] Martin Heusel, Hubert Ramsauer, Thomas Unterthiner, Bernhard Nessler, and Sepp Hochreiter. Gans trained by a two time-scale update rule converge to a local nash equilibrium. *Advances in neural information processing systems*, 30, 2017.

Supplementary Material

5 Proofs

5.1 Proof of Lemma 2

Lemma With a probability of at least τ , we have

$$\sup_{\mathbf{x}, \mathbf{W}} |h(\mathbf{x})| \leq \|\mathbf{w}\|_\infty \sqrt{(DA^2 - \vartheta^2)}, \quad (17)$$

where $A = \sup_{\mathbf{x}} \|\phi(\mathbf{x})\|_2$.

Proof.

$$\begin{aligned} h^2(\mathbf{x}) &= \left(\sum_{i=1}^D w_i \phi_i(\mathbf{x}) \right)^2 \leq \left(\sum_{i=1}^D \|\mathbf{w}\|_\infty \phi_i(\mathbf{x}) \right)^2 = \|\mathbf{w}\|_\infty^2 \left(\sum_{i=1}^D \phi_i(\mathbf{x}) \right)^2 \\ &= \|\mathbf{w}\|_\infty^2 \left(\sum_{i,j} \phi_i(\mathbf{x}) \phi_j(\mathbf{x}) \right) = \|\mathbf{w}\|_\infty^2 \left(\sum_i \phi_i(\mathbf{x})^2 + \sum_{i \neq j} \phi_i(\mathbf{x}) \phi_j(\mathbf{x}) \right) \end{aligned} \quad (18)$$

We have $\|\Phi(\mathbf{x})\|_2 \leq A$. For the first term in equation 18, we have $\sum_m \phi_m(\mathbf{x})^2 \leq A^2$. By using the identity $\phi_m(\mathbf{x})\phi_n(\mathbf{x}) = \frac{1}{2} (\phi_m(\mathbf{x})^2 + \phi_n(\mathbf{x})^2 - (\phi_m(\mathbf{x}) - \phi_n(\mathbf{x}))^2)$, the second term can be rewritten as

$$\sum_{m \neq n} \phi_m(\mathbf{x})\phi_n(\mathbf{x}) = \frac{1}{2} \sum_{m \neq n} \left(\phi_m(\mathbf{x})^2 + \phi_n(\mathbf{x})^2 - (\phi_m(\mathbf{x}) - \phi_n(\mathbf{x}))^2 \right). \quad (19)$$

In addition, we have with a probability τ , $\frac{1}{2} \sum_{m \neq n} (\phi_m(\mathbf{x}) - \phi_n(\mathbf{x}))^2 \geq \vartheta^2$. Thus, we have with a probability at least τ :

$$\sum_{m \neq n} \phi_m(\mathbf{x})\phi_n(\mathbf{x}) \leq \frac{1}{2} (2(D-1)A^2 - 2\vartheta^2) = (D-1)A^2 - \vartheta^2. \quad (20)$$

By putting everything back to equation 18, we have with a probability τ ,

$$G_{\mathbf{W}}^2(\mathbf{x}) \leq \|\mathbf{w}\|_\infty^2 \left(A^2 + (D-1)A^2 - \vartheta^2 \right) = \|\mathbf{w}\|_\infty^2 (DA^2 - \vartheta^2). \quad (21)$$

Thus, with a probability τ ,

$$\sup_{\mathbf{x}, \mathbf{W}} |h(\mathbf{x})| \leq \sqrt{\sup_{\mathbf{x}, \mathbf{W}} G_{\mathbf{W}}^2(\mathbf{x})} \leq \|\mathbf{w}\|_\infty \sqrt{DA^2 - \vartheta^2}. \quad (22)$$

□

5.2 Proof of Lemma 3

Lemma With a probability of at least τ , we have

$$\sup_{\mathbf{x}, \mathbf{y}, h} |E(h, \mathbf{x}, \mathbf{y})| \leq \frac{1}{2} (\|\mathbf{w}\|_\infty \sqrt{(DA^2 - \vartheta^2)} + B)^2. \quad (23)$$

Proof. We have $\sup_{\mathbf{x}, \mathbf{y}, h} |h(\mathbf{x}) - y| \leq \sup_{\mathbf{x}, \mathbf{y}, h} (|h(\mathbf{x})| + |y|) = (\|\mathbf{w}\|_\infty \sqrt{DA^2 - \vartheta^2} + B)$. Thus $\sup_{\mathbf{x}, \mathbf{y}, h} |E(h, \mathbf{x}, \mathbf{y})| \leq \frac{1}{2} (\|\mathbf{w}\|_\infty \sqrt{DA^2 - \vartheta^2} + B)^2$. □

5.3 Proof of Lemma 4

Lemma With a probability of at least τ , we have

$$\mathcal{R}_m(\mathcal{E}) \leq 2D\|\mathbf{w}\|_\infty(\|\mathbf{w}\|_\infty\sqrt{(DA^2 - \vartheta^2)} + B)\mathcal{R}_m(\mathcal{F}) \quad (24)$$

Proof. Using the decomposition property of the Rademacher complexity (if ϕ is a L -Lipschitz function, then $\mathcal{R}_m(\phi(\mathcal{A})) \leq L\mathcal{R}_m(\mathcal{A})$) and given that $\frac{1}{2}\|\cdot - y\|^2$ is K -Lipschitz with a constant $K = \sup_{\mathbf{x}, y, h} \|h(\mathbf{x}) - y\| \leq (\|\mathbf{w}\|_\infty\sqrt{DA^2 - \vartheta^2} + B)$, we have $\mathcal{R}_m(\mathcal{E}) \leq K\mathcal{R}_m(\mathcal{H}) = (\|\mathbf{w}\|_\infty\sqrt{DA^2 - \vartheta^2} + B)\mathcal{R}_m(\mathcal{H})$, where $\mathcal{H} = \{G_{\mathbf{W}}(\mathbf{x}) = \sum_{i=1}^D w_i \phi_i(\mathbf{x})\}$. We also know that $\|\mathbf{w}\|_1 \leq D\|\mathbf{w}\|_\infty$. Next, similar to the proof of Theorem 2.10 in [56], we note that $\sum_{i=1}^D w_i \phi_i(\mathbf{x}) \in (D\|\mathbf{w}\|_\infty)\text{conv}(\mathcal{F} + (-\mathcal{F})) := \mathcal{G}$, where conv denotes the convex hull and \mathcal{F} is the set of ϕ functions. Thus, $\mathcal{R}_m(\mathcal{H}) \leq \mathcal{R}_m(\mathcal{G}) = D\|\mathbf{w}\|_\infty\mathcal{R}_m(\text{conv}(\mathcal{F} + (-\mathcal{F}))) = D\|\mathbf{w}\|_\infty\mathcal{R}_m(\mathcal{F} + (-\mathcal{F})) = 2D\|\mathbf{w}\|_\infty\mathcal{R}_m(\mathcal{F})$. \square

6 Proof of Theorem 1

Theorem For the energy function $E(h, \mathbf{x}, \mathbf{y}) = \frac{1}{2}\|G_{\mathbf{W}}(\mathbf{x}) - y\|_2^2$, over the input set $\mathcal{X} \in \mathbb{R}^N$, hypothesis class $\mathcal{H} = \{h(\mathbf{x}) = G_{\mathbf{W}}(\mathbf{x}) = \sum_{i=1}^D w_i \phi_i(\mathbf{x}) = \mathbf{w}^T \Phi(\mathbf{x}) \mid \Phi \in \mathcal{F}, \forall \mathbf{x} : \|\Phi(\mathbf{x})\|_2 \leq A\}$, and output set $\mathcal{Y} \subset \mathbb{R}$, if the feature set $\{\phi_1(\cdot), \dots, \phi_D(\cdot)\}$ is ϑ -diverse with a probability τ , with a probability of at least $(1 - \delta)\tau$, the following holds for all h in \mathcal{H} :

$$\begin{aligned} \mathbb{E}_{(\mathbf{x}, \mathbf{y}) \sim D}[E(h, \mathbf{x}, \mathbf{y})] &\leq \frac{1}{m} \sum_{(\mathbf{x}, \mathbf{y}) \in \mathcal{S}} E(h, \mathbf{x}, \mathbf{y}) + 4D\|\mathbf{w}\|_\infty(\|\mathbf{w}\|_\infty\sqrt{DA^2 - \vartheta^2} + B)\mathcal{R}_m(\mathcal{F}) \\ &\quad + \frac{1}{2}(\|\mathbf{w}\|_\infty\sqrt{DA^2 - \vartheta^2} + B)^2 \sqrt{\frac{\log(2/\delta)}{2m}}, \end{aligned} \quad (25)$$

where B is the upper-bound of \mathcal{Y} , i.e., $y \leq B, \forall y \in \mathcal{Y}$.

Proof. We replace the variables in Lemma 1 using Lemma 3 and Lemma 4. \square

6.1 Proof of Lemma 5

Lemma With a probability of at least τ , we have

$$\sup_{\mathbf{x}, y, h} |E(h, \mathbf{x}, \mathbf{y})| \leq (\|\mathbf{w}\|_\infty\sqrt{DA^2 - \vartheta^2} + B). \quad (26)$$

Proof. We have $\sup_{\mathbf{x}, y, h} |h(\mathbf{x}) - y| \leq \sup_{\mathbf{x}, y, h} (|h(\mathbf{x})| + |y|) = (\|\mathbf{w}\|_\infty\sqrt{DA^2 - \vartheta^2} + B)$. \square

6.2 Proof of Lemma 6

Lemma With a probability of at least τ , we have

$$\mathcal{R}_m(\mathcal{E}) \leq 2D\|\mathbf{w}\|_\infty\mathcal{R}_m(\mathcal{F}) \quad (27)$$

Proof. $|\cdot|$ is 1-Lipschitz, Thus $\mathcal{R}_m(\mathcal{E}) \leq \mathcal{R}_m(\mathcal{H})$. \square

6.3 Proof of Theorem 2

Theorem For the energy function $E(h, \mathbf{x}, \mathbf{y}) = \|G_{\mathbf{W}}(\mathbf{x}) - y\|_1$, over the input set $\mathcal{X} \in \mathbb{R}^N$, hypothesis class $\mathcal{H} = \{h(\mathbf{x}) = G_{\mathbf{W}}(\mathbf{x}) = \sum_{i=1}^D w_i \phi_i(\mathbf{x}) = \mathbf{w}^T \Phi(\mathbf{x}) \mid \Phi \in \mathcal{F}, \forall \mathbf{x} \|\Phi(\mathbf{x})\|_2 \leq A\}$, and output set $\mathcal{Y} \subset \mathbb{R}$, if the feature set $\{\phi_1(\cdot), \dots, \phi_D(\cdot)\}$ is ϑ -diverse with a probability τ ,

then with a probability of at least $(1 - \delta)\tau$, the following holds for all h in \mathcal{H} :

$$\begin{aligned} \mathbb{E}_{(\mathbf{x}, \mathbf{y}) \sim D} [E(h, \mathbf{x}, \mathbf{y})] &\leq \frac{1}{m} \sum_{(\mathbf{x}, \mathbf{y}) \in \mathcal{S}} E(h, \mathbf{x}, \mathbf{y}) + 4D \|\mathbf{w}\|_\infty \mathcal{R}_m(\mathcal{F}) \\ &\quad + (\|\mathbf{w}\|_\infty \sqrt{DA^2 - \vartheta^2} + B) \sqrt{\frac{\log(2/\delta)}{2m}}, \end{aligned} \quad (28)$$

where B is the upper-bound of \mathcal{Y} , i.e., $y \leq B, \forall y \in \mathcal{Y}$.

Proof. We replace the variables in Lemma 1 using Lemma 5 and Lemma 6. \square

6.4 Proof of Theorem 3

Lemma 7. *With a probability of at least τ , we have*

$$\sup_{\mathbf{x}, \mathbf{y}, h} |E(h, \mathbf{x}, \mathbf{y})| \leq \|\mathbf{w}\|_\infty \sqrt{DA^2 - \vartheta^2}. \quad (29)$$

Proof. We have $\sup -yG_{\mathbf{W}}(\mathbf{x}) \leq \sup |G_{\mathbf{W}}(\mathbf{x})| \leq \|\mathbf{w}\|_\infty \sqrt{DA^2 - \vartheta^2}$. \square

Lemma 8. *With a probability of at least τ , we have*

$$\mathcal{R}_m(\mathcal{E}) \leq 2D \|\mathbf{w}\|_\infty \mathcal{R}_m(\mathcal{F}) \quad (30)$$

Proof. We note that for $y \in \{-1, 1\}$, σ and $-y\sigma$ follow the same distribution. Thus, we have $\mathcal{R}_m(\mathcal{E}) = \mathcal{R}_m(\mathcal{H})$. Next, we note that $\mathcal{R}_m(\mathcal{H}) \leq 2D \|\mathbf{w}\|_\infty \mathcal{R}_m(\mathcal{F})$. \square

Theorem 3 For a well-defined energy function $E(h, \mathbf{x}, \mathbf{y})$ [2], over hypothesis class \mathcal{H} , input set \mathcal{X} and output set \mathcal{Y} , if it has upper-bound M , then with a probability of at least $1 - \delta$, the following holds for all h in \mathcal{H}

$$\begin{aligned} \mathbb{E}_{(\mathbf{x}, \mathbf{y}) \sim D} [E(h, \mathbf{x}, \mathbf{y})] &\leq \frac{1}{m} \sum_{(\mathbf{x}, \mathbf{y}) \in \mathcal{S}} E(h, \mathbf{x}, \mathbf{y}) + 4D \|\mathbf{w}\|_\infty \mathcal{R}_m(\mathcal{F}) \\ &\quad + \|\mathbf{w}\|_\infty \sqrt{DA^2 - \vartheta^2} \sqrt{\frac{\log(2/\delta)}{2m}}, \end{aligned} \quad (31)$$

Proof. We replace the variables in Lemma 1 using Lemma 7 and Lemma 8. \square

6.5 Proof of Theorem 4

Lemma 9. *With a probability of at least $\tau_1\tau_2$, we have*

$$\sup_{\mathbf{x}, \mathbf{y}, h} |E(h, \mathbf{x}, \mathbf{y})| \leq (\mathcal{J}_1 + \mathcal{J}_2) \quad (32)$$

Proof. We have $\|G_{\mathbf{W}}^{(1)}(\mathbf{x}) - G_{\mathbf{W}}^{(2)}(\mathbf{y})\|_2^2 \leq 2(\|G_{\mathbf{W}}^{(1)}(\mathbf{x})\|_2^2 + \|G_{\mathbf{W}}^{(2)}(\mathbf{y})\|_2^2)$. Similar to Theorem 1, we have $\sup \|G_{\mathbf{W}}^{(1)}(\mathbf{x})\|_2^2 \leq \|\mathbf{w}^{(1)}\|_\infty^2 (D^{(1)}A^{(1)2} - \vartheta^{(1)2}) = \mathcal{J}_1$ and $\sup \|G_{\mathbf{W}}^{(2)}(\mathbf{y})\|_2^2 \leq \|\mathbf{w}^{(2)}\|_\infty^2 (D^{(2)}A^{(2)2} - \vartheta^{(2)2}) = \mathcal{J}_2$. We also have $E(h, \mathbf{x}, \mathbf{y}) = \frac{1}{2} \|G_{\mathbf{W}}^{(1)}(\mathbf{x}) - G_{\mathbf{W}}^{(2)}(\mathbf{y})\|_2^2$. \square

Lemma 10. *With a probability of at least $\tau_1\tau_2$, we have*

$$\mathcal{R}_m(\mathcal{E}) \leq 4(\sqrt{\mathcal{J}_1} + \sqrt{\mathcal{J}_2})(D^{(1)}\|\mathbf{w}^{(1)}\|_\infty \mathcal{R}_m(\mathcal{F}_1) + D^{(2)}\|\mathbf{w}^{(2)}\|_\infty \mathcal{R}_m(\mathcal{F}_2)) \quad (33)$$

Proof. Let f be the square function, i.e., $f(x) = \frac{1}{2}x^2$ and $\mathcal{E}_0 = \{G_{\mathbf{W}}^{(1)}(x) - G_{\mathbf{W}}^{(2)}(y) \mid x \in \mathcal{X}, y \in \mathcal{Y}\}$. We have $\mathcal{E} = f(\mathcal{E}_0 + (-\mathcal{E}_0))$. f is Lipschitz over the input space, with a constant L bounded by $\sup_{x, \mathbf{W}} G_{\mathbf{W}}^{(1)}(x) + \sup_{y, \mathbf{W}} G_{\mathbf{W}}^{(2)}(y) \leq \sqrt{\mathcal{J}_1} + \sqrt{\mathcal{J}_2}$. Thus, we have $\mathcal{R}_m(\mathcal{E}) \leq (\sqrt{\mathcal{J}_1} + \sqrt{\mathcal{J}_2})\mathcal{R}_m(\mathcal{E}_0 + (-\mathcal{E}_0)) \leq 2(\sqrt{\mathcal{J}_1} + \sqrt{\mathcal{J}_2})\mathcal{R}_m(\mathcal{E}_0)$. Next, we note that $\mathcal{R}_m(\mathcal{E}_0) = \mathcal{R}_m(\mathcal{H}_1 + (-\mathcal{H}_2)) = \mathcal{R}_m(\mathcal{H}_1) + \mathcal{R}_m(\mathcal{H}_2)$. Using same as technique as in Lemma 4, we have $\mathcal{R}_m(\mathcal{H}_1) \leq 2D^{(1)}\|\mathbf{w}^{(1)}\|_\infty\mathcal{R}_m(\mathcal{F}_1)$ and $\mathcal{R}_m(\mathcal{H}_2) \leq 2D^{(2)}\|\mathbf{w}^{(2)}\|_\infty\mathcal{R}_m(\mathcal{F}_2)$. \square

Theorem 4 For the energy function $E(h, \mathbf{x}, \mathbf{y}) = \frac{1}{2}\|G_{\mathbf{W}}^{(1)}(\mathbf{x}) - G_{\mathbf{W}}^{(2)}(\mathbf{y})\|_2^2$, over the input set $\mathcal{X} \in \mathbb{R}^N$, hypothesis class $\mathcal{H} = \{G_{\mathbf{W}}^{(1)}(\mathbf{x}) = \sum_{i=1}^{D^{(1)}} w_i^{(1)}\phi_i^{(1)}(\mathbf{x}) = \mathbf{w}^{(1)T}\Phi^{(1)}(\mathbf{x}), G_{\mathbf{W}}^{(2)}(\mathbf{y}) = \sum_{i=1}^{D^{(2)}} w_i^{(2)}\phi_i^{(2)}(\mathbf{y}) = \mathbf{w}^{(2)T}\Phi^{(2)}(\mathbf{y}) \mid \Phi^{(1)} \in \mathcal{F}_1, \Phi^{(2)} \in \mathcal{F}_2, \forall \mathbf{x} \|\Phi^{(1)}(\mathbf{x})\|_2 \leq A^{(1)}, \forall \mathbf{y} \|\Phi^{(2)}(\mathbf{y})\|_2 \leq A^{(2)}\}$, and output set $\mathcal{Y} \subset \mathbb{R}^N$, if the feature set $\{\phi_1^{(1)}(\cdot), \dots, \phi_{D^{(1)}}^{(1)}(\cdot)\}$ is $\vartheta^{(1)}$ -diverse with a probability τ_1 and the feature set $\{\phi_1^{(2)}(\cdot), \dots, \phi_{D^{(2)}}^{(2)}(\cdot)\}$ is $\vartheta^{(2)}$ -diverse with a probability τ_2 , then with a probability of at least $(1 - \delta)\tau_1\tau_2$, the following holds for all h in \mathcal{H}

$$\begin{aligned} \mathbb{E}_{(\mathbf{x}, \mathbf{y}) \sim D}[E(h, \mathbf{x}, \mathbf{y})] &\leq \frac{1}{m} \sum_{(\mathbf{x}, \mathbf{y}) \in \mathcal{S}} E(h, \mathbf{x}, \mathbf{y}) \\ &+ 8(\sqrt{\mathcal{J}_1} + \sqrt{\mathcal{J}_2})(D^{(1)}\|\mathbf{w}^{(1)}\|_\infty\mathcal{R}_m(\mathcal{F}_1) + D^{(2)}\|\mathbf{w}^{(2)}\|_\infty\mathcal{R}_m(\mathcal{F}_2)) \\ &+ (\mathcal{J}_1 + \mathcal{J}_2)\sqrt{\frac{\log(2/\delta)}{2m}}, \end{aligned} \quad (34)$$

where $\mathcal{J}_1 = \|\mathbf{w}^{(1)}\|_\infty^2 (D^{(1)}A^{(1)2} - \vartheta^{(1)2})$ and $\mathcal{J}_2 = \|\mathbf{w}^{(2)}\|_\infty^2 (D^{(2)}A^{(2)2} - \vartheta^{(2)2})$.

Proof. We replace the variables in Lemma 1 using Lemma 9 and Lemma 10. \square

7 Additional experiments

7.1 Additional experiments: Image Generation Example with MNIST

Besides the experiments in the paper, we present here additional experiments with the proposed regularizer. Recently, there has been a high interest in using EBMs to solve image/text generation tasks [57, 58, 20, 11]. In this subsection, we validate the proposed regularizer on the simple example of MNIST digits image generation, as in [57]. For the EBM model, we use a simple CNN model composed of four convolutional layers followed by a linear layer. The training protocol is the same as in [59, 57], i.e., using Langevin dynamics Markov chain Monte Carlo (MCMC) and a sampling buffer to accelerate training.

For the EBM model, we used a simple CNN model composed of four convolutional layers followed by a linear layer. The full CNN model is presented in Table 3. The training protocol is the same as in [59, 57], i.e., using Langevin dynamics MCMC and a sampling buffer to accelerate training. All models were trained for 60 epochs using Adam optimizer with learning rate $lr = 1e - 4$ and a batch size of 128.

In this example, the features, i.e., the latent representation obtained at the last intermediate layer, are learned in an end-to-end way. We evaluate the performance of our approach by augmenting the contrastive divergence loss using equation 15 to penalize the feature redundancy. We quantitatively evaluate the image quality of EBMs with ‘Fréchet Inception Distance’ (FID) score [60] and the negative log-likelihood (NLL) loss in Table 4 for different values of β . We note that we obtain consistently better FID and NLL scores by penalizing the similarity of the learned features. The best performance is achieved by $\beta = 1e^{-13}$, which yields more than 10%, in terms of FID, improvement compared to the original EBM model.

To gain insights into the visual performance of our approach, we plot a few intermediate samples of the MCMC sampling (Langevin Dynamics). The results obtained by the EBM with $\beta = 1e^{-13}$ are presented in Figure 4. Initiating from random noise, MCMC obtains reasonable figures after only 64 steps. The digits get clearer and more realistic over the iterations.

Layer	Output shape
Input	[1,28,28]
Cov (16 5 × 5)	[16,16,16]
Swish activation	[16,16,16]
Cov (32 3 × 3)	[32,8,8]
Swish activation	[32,8,8]
Cov (64 3 × 3)	[64,4,4]
Swish activation	[64,4,4]
Cov (64 3 × 3)	[64,2,2]
Swish activation	[64,2,2]
Flatten	[256]
Linear	[64]
Swish activation*	[64]
Linear	[1]

Table 3: Simple CNN model used in the example. * refers to the features' layer.

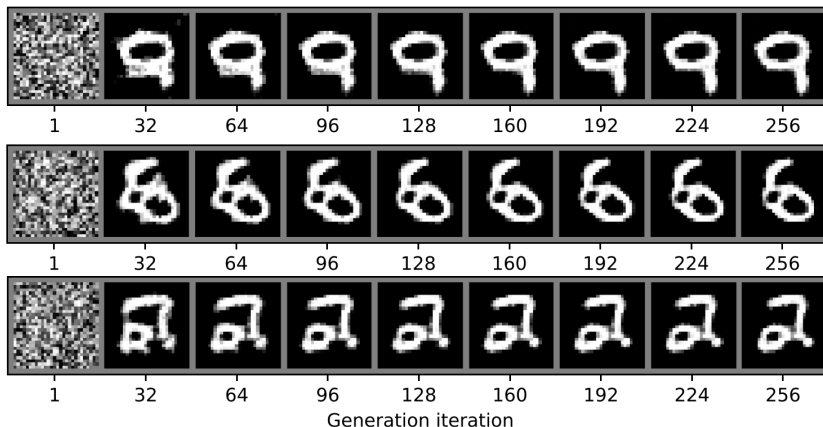


Figure 4: Qualitative results of our approach ($\beta = 1e^{-13}$): Few intermediate samples of the MCMC sampling (Langevin Dynamics).

In addition to the visual results in Figure 4, Figure 5 presents additional qualitative results. For the first two examples (top ones), the model is able to converge to a realistic image within a reasonable amount of iterations. For the last two examples (at the bottom), we present failure cases of our approach. For these two tests, the generated image still improves over iterations. However, the model failed to converge to a clear realistic MNIST image after 256 steps.

Approach	FID	NLL loss
EBM	0.0109 ± 0.0004	0.7112 ± 0.0190
ours ($\beta = 1e^{-11}$)	0.0107 ± 0.0004	0.7109 ± 0.0111
ours ($\beta = 1e^{-12}$)	0.0104 ± 0.0003	0.7105 ± 0.0112
ours ($\beta = 1e^{-13}$)	0.0099 ± 0.0006	0.7108 ± 0.0111

Table 4: Table of FID scores and negative log-likelihood (NLL) loss of different approaches for generations of MNIST images. Each experiment was performed three times with different random seeds, the results are reported as the mean/SEM over these runs.

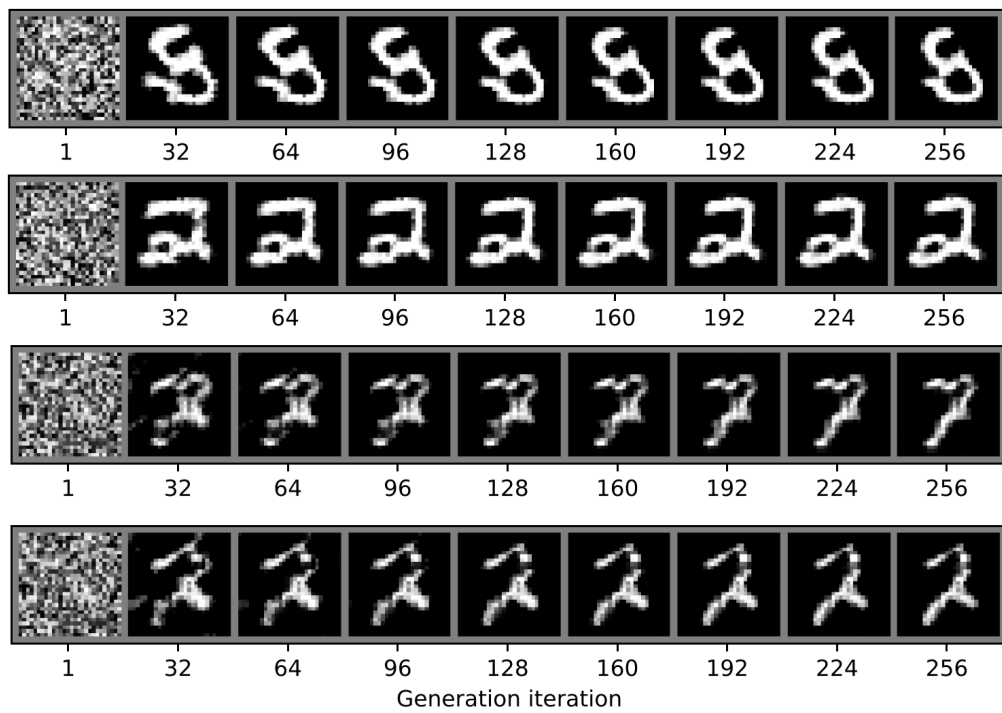


Figure 5: Qualitative results of EBM augmented with our regularizer with $\beta = 1e^{-13}$: Few intermediate samples of the MCMC sampling (Langevin Dynamics).